

## Supplementary Materials

# Propelling Solar-to-H<sub>2</sub>O<sub>2</sub> Conversation of Molecularly Tunable Covalent Heptazine Skeleton with Boosted Spatial Charge Separation and Awakened n-π\* Electron Transition

Yuhan Yan<sup>a,c</sup>, Liang Wang<sup>a,c,\*</sup>, Tianyu Zhou<sup>a,b,\*</sup>, Jiaqi Sun<sup>a,c</sup>, Jihan Zhao<sup>a,c</sup>,  
Dongshu Sun<sup>a,c</sup>, Chunbo Liu<sup>a,c,\*</sup>, Bo Hu<sup>a,b,c</sup>, Guangbo Che<sup>a</sup>

a Key Laboratory of Preparation and Application of Environmental Friendly  
Materials, Ministry of Education, College of Chemistry, Jilin Normal University,  
Changchun 130103, P.R. China

b Jilin Joint Technology Innovation Laboratory of Developing and Utilizing  
Materials of Reducing Pollution and Carbon Emissions, College of Engineering, Jilin  
Normal University, Siping 136000, P.R. China

c The Joint Laboratory of Intelligent Manufacturing of Energy and Environmental  
Materials, Jilin Normal University, Siping, 136000, P. R. China.

---

\* Corresponding authors: Liang Wang (wangliang7469@163.com), Tianyu Zhou (tianyuzhou@jlnu.edu.cn),  
Chunbo Liu (chunboliu@jlnu.edu.cn).

## Table of Contents

### 1. Materials (3)

### 2. Characterizations (3)

### 3. Theoretical calculations (3)

### 4. Charts (5-12)

**Fig. S1** SEM EDS mapping of 30-P-KPHI. ....(5)

**Fig. S2** N<sub>2</sub> adsorption-desorption and pore size distributions (inset)  
curves of CN and 30-P-KPHI. ....(6)

**Video data** Water contact angle diagram of CN and 30-P-KPHI. ....(7)

**Table S1** Surface elemental composition of CN and 30-P-KPHI based  
on XPS. ....(8)

**Table S2** Related reports on photocatalytic H<sub>2</sub>O<sub>2</sub> production. ....(9)

**Fig.S3** Cyclic experiment of 30-P-KPHI in the photocatalytic  
preparation of H<sub>2</sub>O<sub>2</sub> (a). XRD (b) and FT-IR (c) before and after  
five cycles. ....(10)

**Fig. S4** LSV curves of CN and 30-P-KPHI.....(11)

### 5. References (12-13)

## **1.Materials**

Urea, 2,4-Pyridinedicarboxylic acid, Lithium chloride, potassium hydrogen phthalate were bought from Aladdin Reagent Co., Ltd. Potassium chloride, potassium iodide, p-benzoquinone, tert-butanol and EDTA-2Na were purchased from Macklin Chemical Reagent Co., Ltd.

## **2.Characterizations**

The crystalline phase of photocatalysts were investigated by X-ray diffraction (XRD, RIGAKU, D/max-2500). The functional groups of all samples were studied by fourier transform infrared spectroscopy (FTIR, thermoscientific Nicolet 4700). The structure and morphology were tested by field emission scanning electron microscopy (FESEM, Hitachi regulus 8100), transmission electron microscopy (TEM, JEM-2100F) and atomic force microscopy (AFM, Brooke dimension Icon). X-ray photoelectron spectroscopy (XPS) and UV-vis diffuse reflectance spectrum (UV-vis DRS) were obtained by ESCALAB250XI electronic spectrometer (VG scientific, USA) and Cary 500 spectrometer (Shimadzu UV-2550, Japan). Photoluminescence (PL), time-resolved PL (TR-PL) spectra, photocurrent response (PCR), electrochemical impedance spectroscopy (EIS) and electron spin resonance (EPR) were characterized by F4500 (Hitachi, Japan) photoluminescence detector, IBH-TemPro (HORIBA JobinYvon, France), CHI760E electrochemical workstation (Shanghai Chenhua Instrument Co., Ltd.), PGSTAT-302N (metrohm China Ltd.) electrochemical workstation and Brooke A300 (Germany) respectively.

## **3.Theoretical calculations**

All calculations were carried out with the Gaussian 16 software [1]. Density functional theory (DFT) calculations were carried out with the B3LYP functional [2] with the combination of Grimme's D3B [3] dispersion correction. The basis set of 6-31G (d,p) was adopted for the geometry optimization and frequency calculations. The geometries were fully optimized without any structural constraints. The harmonic frequency calculations were carried out at the same level of theory to verify that all

structures have no imaginary frequency. The molecular orbitals figures and electrostatic potential surfaces were extracted from the Multiwfn 3.8 program [4] and visualized using the visual molecular dynamics (VMD) [5] software. The final energies for the fully optimized structures were calculated with the larger 6-311G (d, p) basis set. The binding energy ( $E_b$ ) was calculated by the following equation:

$$E_b = E_{\text{Complex}} - (E_{M1} + E_{M2}) \quad (1)$$

where  $E_{\text{Complex}}$ ,  $E_{M1}$ , and  $E_{M2}$  represent the energies of the complex, and energies of the interacting molecules, respectively.

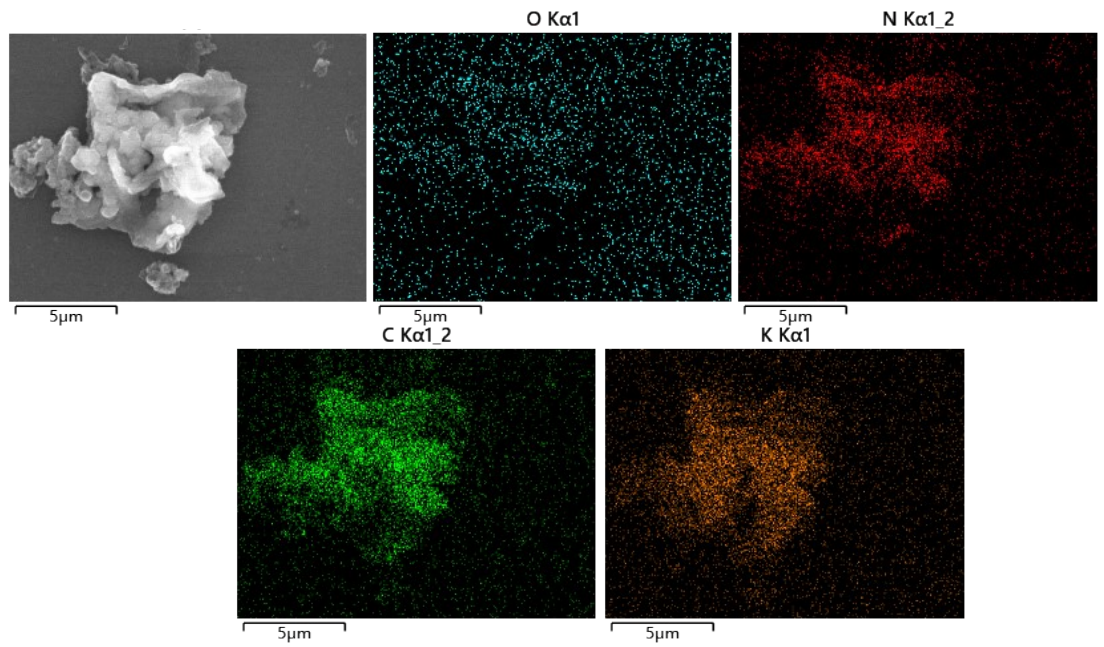


Fig. S1 SEM EDS mapping of 30-P-KPHI.

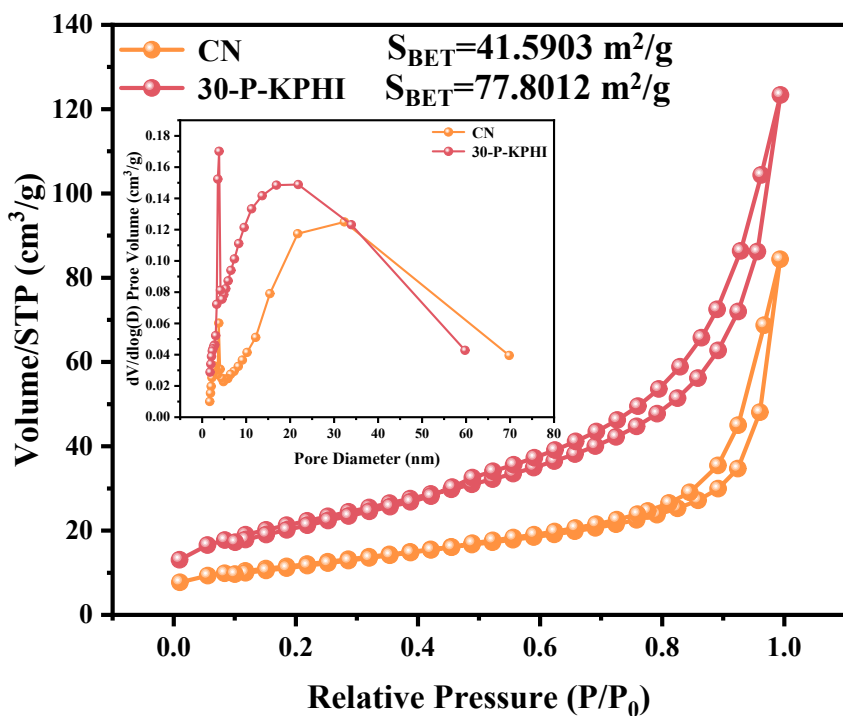


Fig. S2 N<sub>2</sub> adsorption-desorption and pore size distributions (inset) curves of CN and 30-P-KPHI.



CN.mp4



30-P-KPHI.mp4

Video data Water contact angle diagram of CN and 30-P-KPHI.

Table S1 Surface elemental composition of CN and 30-P-KPHI based on XPS.

Catalyst	C (atom %)	N (atom %)	O (atom %)	K (atom %)	Li (atom %)	C/N
CN	75.14	15.8	9.06	—	—	4.76
30-P-KPHI	60.89	8.28	11.09	12.91	6.83	7.35

Table S2 Related reports on photocatalytic H<sub>2</sub>O<sub>2</sub> production.

Catalysts	Reaction solution	Irradiation conditions	H <sub>2</sub> O <sub>2</sub> production rate (μmol·g <sup>-1</sup> ·h <sup>-1</sup> )	Ref.
DCNS	10% ethanol	300 W Xe lamp	3080	[6]
KDCN-0.2	10% isopropanol	300 W Xe lamp	557.8	[7]
SCN5	10% isopropanol	300 W Xe lamp	703.4	[8]
ACN	10% isopropanol	300 W Xe lamp	1874	[9]
Ni <sub>4%</sub> /O <sub>0.2</sub> tCN	10% ethanol	300 W Xe lamp	2464	[10]
0.6% PDI/CNA	10% isopropanol	400 nm ≤ λ ≤ 760 nm	1605	[11]
C <sub>3</sub> N <sub>4</sub> /NiIn <sub>2</sub> S <sub>4</sub>	10% ethanol	300 W Xe lamp	2700	[12]
H-CN	10% isopropanol	300 W Xe lamp	718.4	[13]
1.0 ZIS/CN	10% isopropanol	AM 1.5, 100 mW cm <sup>-2</sup>	854.7	[14]
MPCN	10% isopropanol	300 W Xe lamp	4424	[15]
DDCN	10% methanol	λ ≥ 420 nm	1031	[16]
<b>30-P-KPHI</b>	<b>10% ethanol</b>	<b>300 W Xe lamp</b>	<b>5566</b>	<b>This work</b>

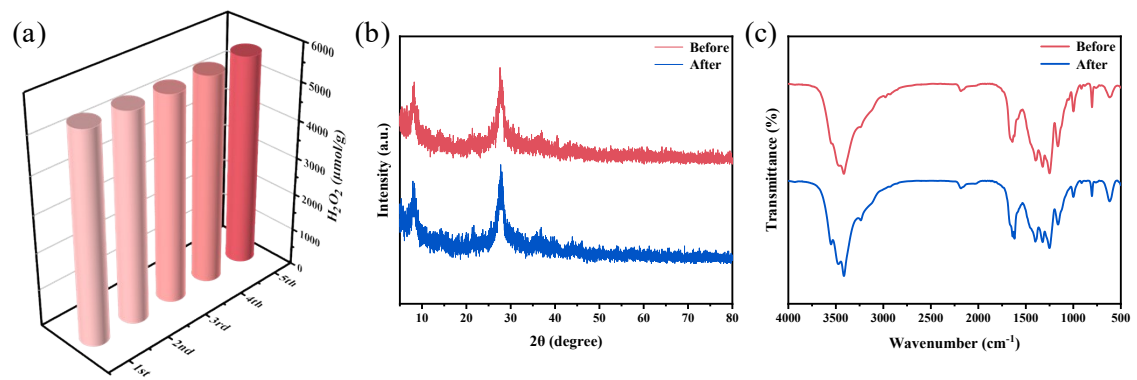


Fig. S3 Cycling photocatalytic  $H_2O_2$  production of 30-P-KPHI (a). XRD (b) and FTIR (c) of 30-P-KPHI before and after circulation.

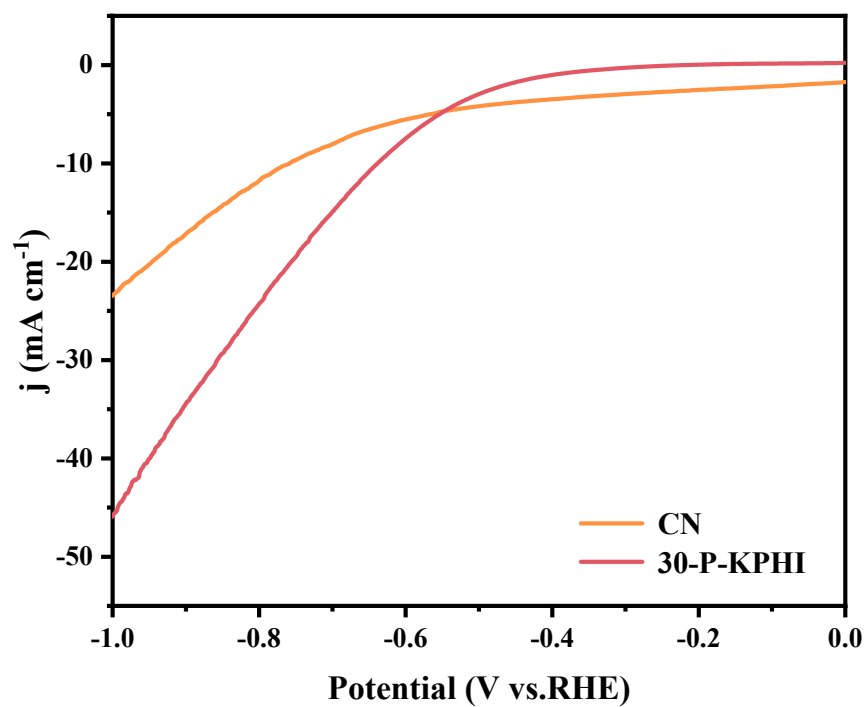


Fig. S4 LSV curves of CN and 30-P-KPHI.

## 5. References

- [1] Frisch, M. J., Trucks, G. W., Schlegel, H. B., Scuseria, G. E., Robb, M. A., Cheeseman, J. R., Scalmani, G., Barone, V., Petersson, G. A., Nakatsuji, H., Li, X., Caricato, M., Marenich, A. V., Bloino, J., Janesko, B. G., Gomperts, R., Mennucci, B., Hratchian, H. P., Ortiz, J. V., Izmaylov, A. F., Sonnenberg, J. L., Williams-Young, D., Ding, F., Lippiani, F., Egidi, F., Goings, J., Peng, B., Petrone, A., Henderson, T., Ranasinghe, D., Zakrzewski, V. G., Gao, J., Rega, N., Zheng, G., Liang, W., Hada, M., Ehara, M., Toyota, K., Fukuda, R., Hasegawa, J., Ishida, M., Nakajima, T., Honda, Y., Kitao, O., Nakai, H., Vreven, T., Throssell, K., Montgomery Jr., J. A., Peralta, J. E., Ogliaro, F., Bearpark, M. J., Heyd, J. J., Brothers, E. N., Kudin, K. N., Staroverov, V. N., Keith, T. A., Kobayashi, R., Normand, J., Raghavachari, K., Rendell, A. P., Burant, J. C., Iyengar, S. S., Tomasi, J., Cossi, M., Millam, J. M., Klene, M., Adamo, C., Cammi, R., Ochterski, J. W., Martin, R. L., Morokuma, K., Farkas, O., Foresman, J. B., Fox, D. J. Gaussian 16 Rev. A.01, *Wallingford, CT*, 2016.
- [2] Becke, A. D., *J. Chem. Phys.*, 1993, **98**, 5648-5652.
- [3] Grimme, S., Ehrlich, S., Goerigk, L., *J. Comput. Chem.*, 2011, **32**, 1456-1465.
- [4] Lu, T., Chen, F., *J. Comput. Chem.*, 2012, **33**, 580-592.
- [5] Humphrey, W., Dalke, A., Schulter, K., *J. Molec. Graphics*, 1996, **14**, 33-38.
- [6] Q. He, B. Viengkeo, X. Zhao, Z.Y. Qin, J. Zhang, X.H. Yu, Y.P. Hu, W. *Nano Res.*, 2023, **16**, 4524-4530.
- [7] Y. Pan, X.J. Liu, W. Zhang, B.B. Shao, Z.F. Liu, Q.H. Liang, T. Wu, Q.Y. He, J. Huang, Z. Peng, Y. Liu, C.H. Zhao, *Chem. Eng. J.*, 2022, **427**, 132032.
- [8] C.C. Chu, W. Miao, Q.J. Li, D.D. Wang, Y. Liu, S. Mao, *Chem. Eng. J.*, 2022, **428**, 132531.
- [9] Y.M. Zheng, Y. Luo, Q.S. Ruan, S.H. Wang, J. Yu, X.L. Guo, W.J. Zhang, H. Xie, Z. Zhang, Y. Huang, *Appl. Catal. B*, 2022, **311**, 121372.
- [10] R.F. Du, K. Xiao, B.Y. Li, X. Han, C.Q. Zhang, X. Wang, Y. Zuo, P. Guardia, J.S. Li, J.B. Chen, J., *Chem. Eng. J.*, 2022, **441**, 135999.

- [11] J.D. Hu, C. Chen, H.B. Yang, F.Y. Yang, J.F. Qu, X.G. Yang, W. Sun, L.M. Dai, C.M. Li, *Appl. Catal. B*, 2022, **317**, 121723.
- [12] A.H. Wang, H.G. Liang, F. Chen, X.L. Tian, S.B. Yin, S.Y. Jing, P. Tsakaras, *Appl. Catal. B*, 2022, **310**, 121336.
- [13] Z. Zhang, Y.M. Zheng, H. Xie, J.J. Zhao, X.L. Guo, W.J. Zhang, Q.P. Fu, S.H. Wang, Q. Xu, Y. Huang, *J. Alloy. Compd.*, 2022, **904**, 164028.
- [14] Y.Y. Shao, J.D. Hu, T.Y. Yang, X.G. Yang, J.F. Qu, Q. Xu, C.M. Li, *Carbon*, 2022, **190**, 337-347.
- [15] Yuan J, Tian N, Zhu Z, Yu W, Li M, Zhang Y, Huang H. *Chem. Eng. J.*, 2023, **467**.
- [16] Ba GM, Hu HL, Bi FH, Yu JB, Liu EZ, Ye JH, Wang DF. *Appl Catal B*, 2025, **361**, 11.